Dean, L. E., D. R. Moran, and R. D. Hicks, 2022: In-situ video observations and analysis of the 16 June 2014 Pilger, Nebraska EF4 west tornado. *Electronic J. Severe Storms Meteor.*, **17** (3), 1–28.

Electronic Journal of SEVERE STORMS METEOROLOGY

In-Situ Video Observations and Analysis of the 16 June 2014 Pilger, Nebraska EF4 West Tornado

LANNY E. DEAN
WeatherBug, PACRITEX, Rogersville, Missouri

DAVID R. MORAN
DTN, PACRITEX, Yukon, Oklahoma

RANDY D. HICKS
PACRITEX, Cave Springs, Missouri

(Submitted 2 June 2022; in final form 30 November 2022)

ABSTRACT

An unusual event involving two large and violent EF4 tornadoes occurring simultaneously impacted the Pilger, NE area on 16 June 2014, resulting in two deaths. A privately funded scientific field campaign successfully obtained in-situ video observations inside the westernmost tornado prior to its striking the town of Pilger. The results resolve fine details of the tornado core wind field, which are presented and discussed, including several important or unique observations not previously documented within existing in-situ tornado video research. These include documentation of many subvortices (as many as nine concurrently at one point) evolving and dissolving on the order of seconds or fractions of seconds while rotating about a concentric axis. A single but separate independent vortex was located on the outside rim of the parent tornado core, and observations confirm tornadic damage well outside the visible parent tornado vortex. This study also adds to the small number of tornado cases documented using in-situ observations as a reference for further research.

1. Introduction

Documenting in-situ observations in tornado core wind fields has proven very difficult during years of field study (Samaras 2006). Field projects such as Verification of the Origins of Rotation in Tornadoes Experiment (VORTEX; Rasmussen et al. 1994), Tactical Weather Instrumented Sampling in Tornadoes Experiment (Twistex; Karstens et al. 2008), and recently, Tornado Winds from In-situ and Radars at Low-level (TWIRL; Kosiba and Wurman 2016), have shown to be very beneficial in helping to bridge the gap between in-situ observations and radar-based resolutions of tornadoes and tornadic supercells. Past in-situ tornado research primarily has concentrated on pressure deficits with one of the most notable in-situ data sets gathered by the late Tim Samaras, where a 100-hPa pressure deficit was documented near Manchester, SD (Lee et al. 2004). A fortuitous encounter with the 21 April 2007 Tulia, TX tornado resulted in likely the largest in-situ tornado pressure deficit observation known to date, where a 194-hPa pressure deficit was measured (Blair et al. 2008). While both the Lee and Blair publications discuss video observations, the Blair literature highlights a video observation just after being struck by the Tulia, TX tornado (their Fig. 8). The authors believe the Tulia video observation to be near in-situ as the tornado was already some distance from the observers and moving away from them. Therefore, it is unclear if any intentional in-situ video observations were documented during these distinguished events.

Corresponding author address: Lanny E. Dean, PACRITEX, 167 Cody Dr. Rogersville, Missouri 65742. E-mail: led42@msstate.edu

Numerous unintentional in-situ video observations have been documented over the last decade by storm chasers and broadcast meteorologists, with likely the most notable on 31 May 2013, when a media crew penetrated the El Reno, OK EF3 tornado, injuring the occupants (Wurman et al. 2014, hereafter W14). Although these accidental in-situ documentation are certainly noteworthy, they have resulted in little formal literature. Except for research work by Samaras (Karstens et al. 2010; Lee et al. 2011) and Wurman et al. (2013), who successfully used a tornado-intercept vehicle (TIV) to document in-situ video during the 5 June 2009 Goshen County, WY tornado, few other intentional in-situ video datasets have been published.

This paper will reveal successful ground-based intentional in-situ video observations with analysis and unique observations of the Pilger, NE EF4 west tornado. While the Pilger, NE tornado event resulted in two violent EF4 tornadoes occurring simultaneously, and three additional violent tornadoes occurring across northeast Nebraska, this case study focuses only on the in situ and visual observations from the westernmost Pilger, NE tornado (hereafter the Pilger west tornado, Fig. 1).

Figure 1: Pilger, NE, western-most tornado attaining wedge shape on 16 June 2014. Video screen capture by Randy Hicks. *Click image to enlarge.*

An overview of the meteorological and convective event is provided in Section 2. Section 3 describes the privately funded field research campaign and detailed probe instrumentation. Visual observations (non-probe) are detailed in section 4. Section 5 showcases the in-situ observations, tornado evolution, and analysis. Future work is highlighted in section 6. The paper concludes with a summary and detailed discussion of the results presented in section 7.

2. Meteorological and convective overview

During the afternoon of 16 June 2014, numerous severe thunderstorms developed from Wisconsin through northern Iowa into Nebraska due in part to a strengthening upper trough over the western U.S. From morning upper-air observations, a midlevel speed max was approaching the Central and Northern Plains from the Great Basin region, increasing strong southwesterly flow aloft and helping to provide broad forcing for ascent as well as enhancing vertical wind shear (Fig. 2a). In lower levels, a strong southerly jet was evident across Kansas and Nebraska (Fig. 2b), advecting greater moisture content northward through the Plains.

By early afternoon at the surface, a cyclone was deepening over southwest South Dakota into northwest Nebraska along a northward moving warm front (Fig. 3). Also seen in Fig. 3, morning convection had initiated an arcing west-east outflow boundary (hereafter OFB) over northeastern Nebraska that began to move back northward in the strong low-level flow during the afternoon. Convergence near and north of the OFB (Fig. 4) helped to provide a primary focus area for the initiation of deep moist convection, which enhanced an environment already favorable for severe weather, including supercells and tornadoes.

The mesoscale environment across eastern Nebraska on the afternoon of 16 June 2014 was characterized by extreme instability and strong wind shear. A 1900 UTC special sounding released from the NWS in Omaha/Valley, NE (Fig. 5) highlighted most unstable (MU) CAPE >5700 J kg^{-1} in the warm sector, near and south of the OFB. Strong directional and speed shear near 50 kt (26 m s^{-1}) also was observed through 3 km, with 0–1-km storm-relative helicity (SRH) nearing 400 m^2 s^{-2}. Also in Fig. 5, the effective bulk wind difference (EBWD) is 60 kt (31 m s^{-1}) with 528 m^2 s^{-2} effective storm-relative helicity (ESRH, EBWD; Thompson et al. 2007, hereafter T07). The T07 research shows EBWD effectively discriminated between supercell and nonsupercell storms, with ESRH a better discriminator between weak and significant tornado environments, compared to 0–1-km SRH. For perspective, the observed ESRH from the 16 June 2014 1900 UTC sounding lies above the 10th percentile of the T07 significant-tornado ESRH distribution (their Fig. 8), highlighting the rarity of the kinematic environment.

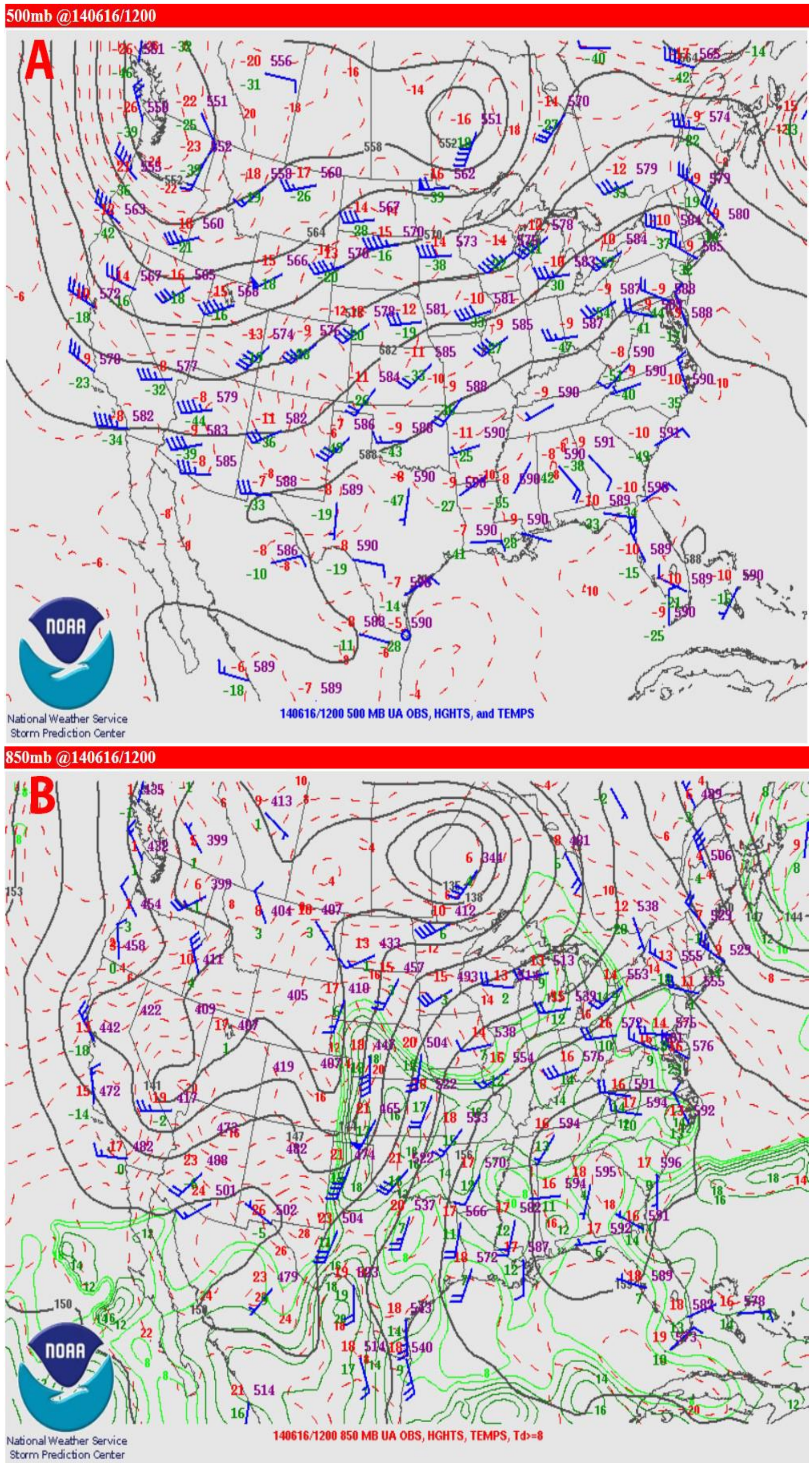

Figure 2: Objective upper-air analysis valid 1200 UTC 16 June 2014. Geopotential heights at a) 500 hPa and b) 850 hPa. Standard station model in conventional abbreviated format. Images courtesy Storm Prediction Center, 2014.

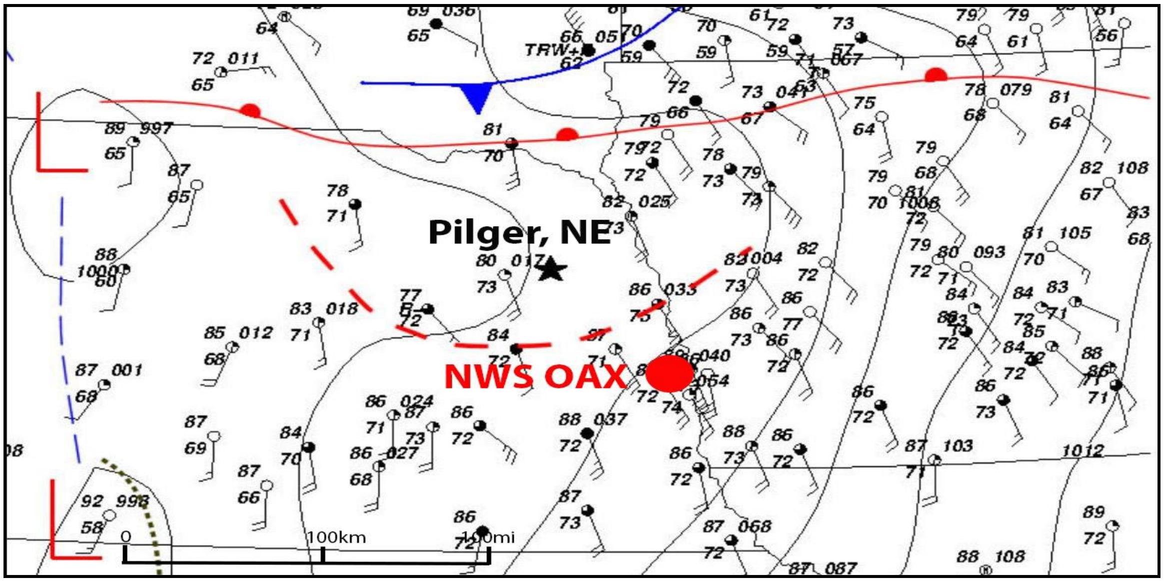

Figure 3: Subjective surface analysis valid 2000 UTC 16 June 2014. Conventional frontal features and station plots. Outflow boundary delineated with a dashed red line. The black star denotes approximate location of Pilger, NE; red circle denotes approximate location of sounding site listed as NWS OAX. Base image from NWS Omaha/Valley, NE.

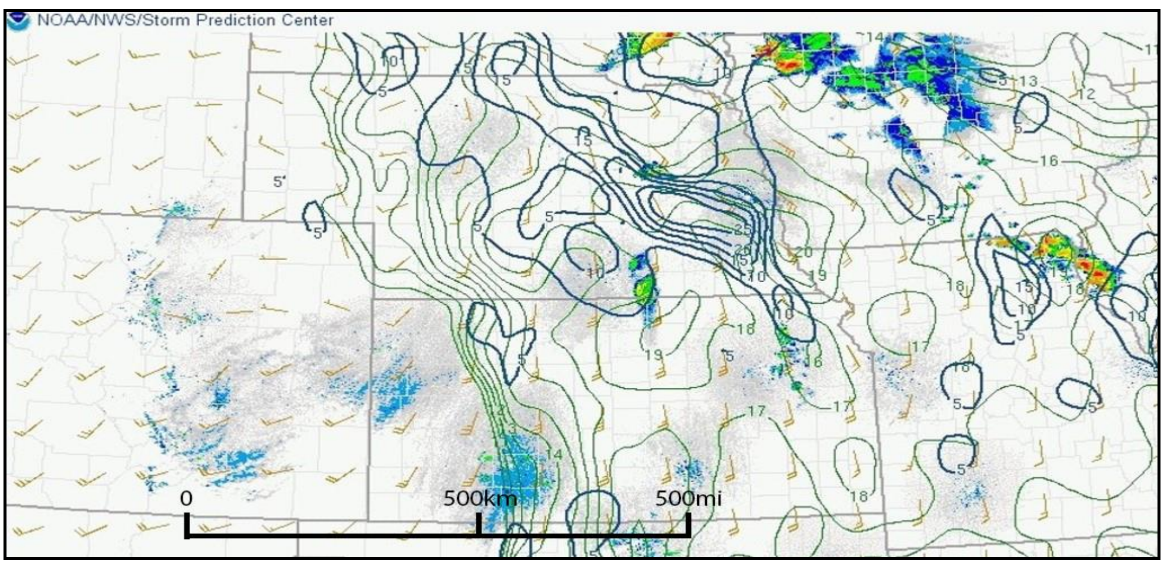

Figure 4: Objective surface analysis valid 1900 UTC 16 June 2014. Moisture convergence (blue lines) and mixing ratio (green lines). Image courtesy Storm Prediction Center, 2014.

Convective initiation occurred near 1900 UTC, with storms maturing into a supercell by 2030 UTC southwest of Stanton, NE (Fig. 6), ~75 km northwest of the sounding site. The first tornado was reported around 2040 UTC 8 mi (12.8 km) south of Norfolk, NE (Fig. 6). Based on tornado track data from the NWS Omaha/Valley, NE (https://www.weather.gov/oax/event_archive_20140616), and storm chasers, this cyclic supercell produced five tornadoes, four of which were rated EF4 (Fig. 6), with the two tornadoes near Pilger causing 2 deaths. The Pilger west tornado (the focus of this paper) developed near 2109 UTC east of Stanton, NE, and grew in both size and intensity into a large EF4 tornado that later struck Pilger, resulting in 1 fatality.

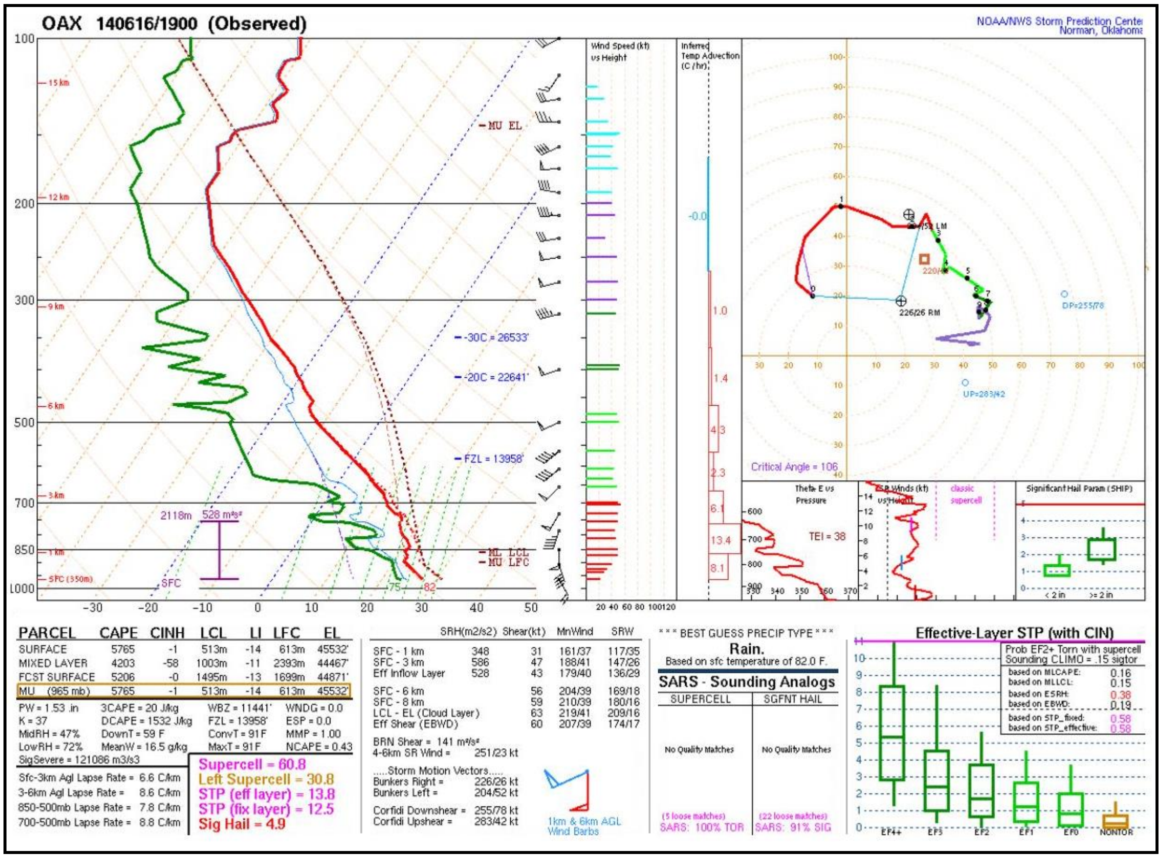

Figure 5: Observed special skew *T*–log*p* sounding diagram and hodograph from NWS Omaha/Valley, NE, 1900 UTC 16 June 2014, shows the combination of extreme instability and strong vertical wind shear. Image courtesy Storm Prediction Center, 2014. *Click image to enlarge.*

3. PACRITEX

The Pressure Acoustics Recordings Inside Tornadoes Experiment (hereafter PACRITEX) is a privately funded field research campaign initiated in 2012. The multifaceted objectives of the PACRITEX field research include obtaining in-situ infrasonic signatures, pressure deficit, and videographic data in and near tornado cores and supercells. The loss of the late Tim Samaras and the valuable scientific work of TWISTEX (Lee et al. 2011) ceased in 2013, left a void within the in-situ tornado research field. The PACRITEX core mission is to help fill this void by continuing similar types of in-situ tornado research, including the study of infrasonic signatures (i.e., inaudible frequency signatures within the 0.5–10-Hz frequency range; Bedard 2005) before and during tornadogenesis.

a. Ground-based probes

PACRITEX field research equipment includes a total of six conical flat-top probes. Each respective probe houses various meteorological sensors, camera equipment, infrasonic data loggers, GPS, and a quad-core 1.2-GHz Broadcom CPU data logger. All ground-based probes are conically shaped with a flat-top design and were constructed from 4.8-mm (3/16 in) thick plate steel (Fig. 7).

The PACRITEX probe housings were built utilizing the Samaras' Hardened In-situ Tornado Pressure Recorder (hereafter, HITPR) design (Samaras and Lee 2003, hereafter SL03), with differences in the fabrication build of the flat-top design instead of the conical top design to allow for an upward facing camera mount on top of the probes. While each probe housing resembled

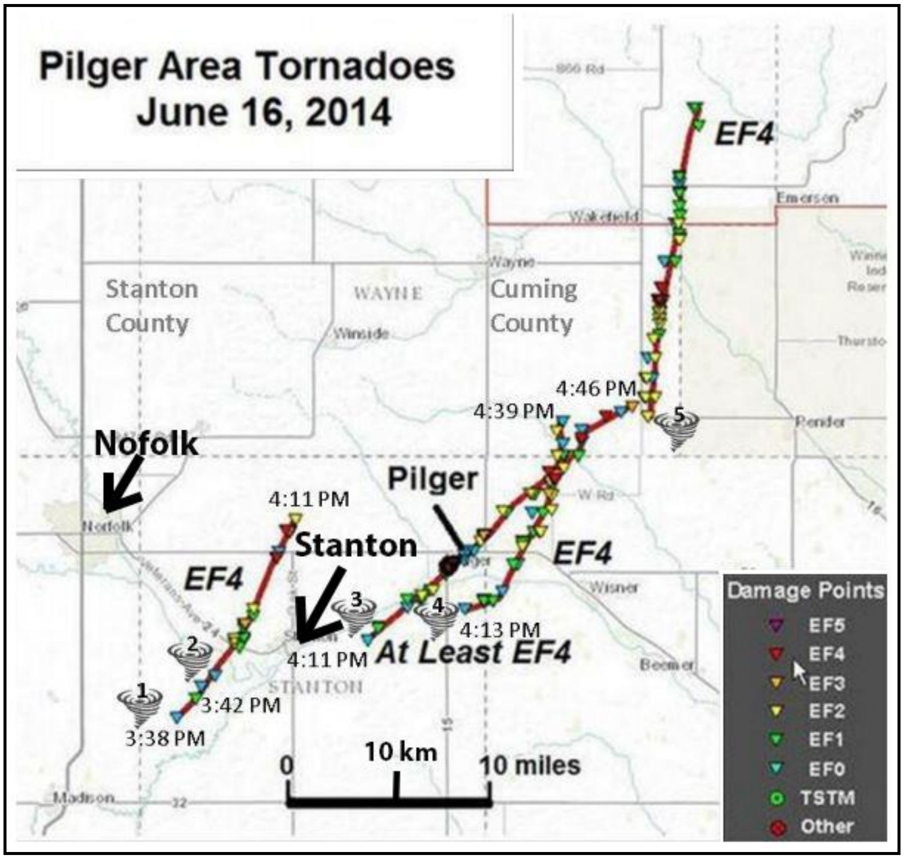

Figure 6: Map of Pilger, NE area tornado tracks, time, and ratings from 16 June 2014. Base image from NWS in Omaha/Valley, NE.

Figure 7: PACRITEX probe showing 4.7-mm steel plating and internal electronic data-logging equipment.

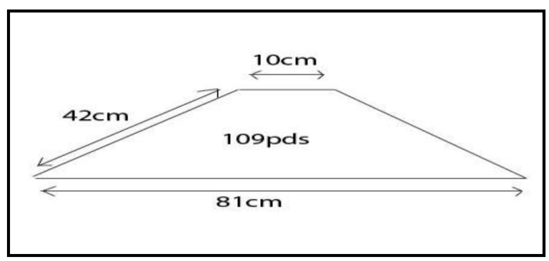

Figure 8: Schematic of PACRITEX probe.

Samaras' original HITPR in shape, specific concentration was placed on the weight and size with respect to the flat-top design. The conical flat-top probes have a base circumference of 81 cm and a top circumference of 10 cm, and weigh 49.4 kg (Fig. 8).

Two of the six ground probes were utilized as video probes only, with fabricated indent shadow boxes housing two GoPro Hero2 cameras on two sides of the probe and a top-mounted GoPro Hero2 camera, for a total of three cameras (Fig. 9). Each probe camera has a 1-2/5 CMOS 11MP sensor with an F/2.8 fixed lens and a 170° field of view (hereafter, FOV). All camera video recording resolution was set at 1920 × 1080P while recording at 30 frames per second (FPS).

b. Probe-testing validation

Lack of access to a wind tunnel or trip bar device limited testing of the probe housing designs in a controlled environment. This proved problematic concerning any ground boundary layer effects on the probe housings. Due to the volatile tornado boundary layer (Kosiba and Wurman 2013), all probe fabrication assumed that the ground boundary-layer effects would vary from those of a conical top design, such as the Samaras HITPR with a known 22.7-kg weight. Thus, lofting or sliding possibilities might exist unless the overall weight of the probe was increased. Using SL03 "Moments, Lift, and Drag" testing results as a base (SL03 Figs. 10–12), PACRITEX probe fabrication increased the overall probe weight to 49.4 kg, more than double HITPR weight. Validating the exact lofting or sliding forces independent of boundary-layer type was antecedent to any such thick or thin boundary-layer effects study. Considering the PACRITEX probe housings differed mainly in size and weight from that of HITPR, the increase in weight and size with the flat-top design would negate any lofting or sliding concerns. With limited funding, all equipment testing had to be done in-field during severe weather and storm chase seasons. This included deploying the probes near and in the chaotic tornado-core flow fields without wind tunnel or trip-bar survivability.

Figure 9: PACRITEX video probe with flat-top design, shadow boxes, and video cameras attached test results. Simply stated, a probe would need to be placed inside the tornado core to see if it would survive.

The first successful probe deployment survivability test during the PACRITEX field research campaign came on 16 June 2014, during the Pilger, NE EF4 west tornado. A ground-based video probe was placed in the direct path of the Pilger west tornado and successfully recorded in-situ video from just inside the northern periphery of the tornado core flow field (Fig. 10). The video probe did not loft, slide or turn as validated by the three separate video camera recordings. Retrieval of the video probe also validated that the "FRONT and REAR" facing logo/lettering (Fig. 9) was not displaced from the original westerly/easterly facing deployment position.

Figure 10: Video screen capture of the Pilger, NE tornado starting to impact the PACRITEX video probe. *Click image to enlarge.*

4. Visual observations (non-probe)

Two support vehicles (hereafter SV1 and SV2) were used to support the probe deployment team (hereafter DT) during the Pilger in-situ deployment. The first visual sign of rotation leading up to the Pilger west tornado was observed by SV2, roughly 3 mi (4.8 km) east of Stanton, NE, at 2056:10 UTC. SV2 turned north on 569th Ave. from 835½ Rd (41.9392N, −97.1560W) to document the assumed rotation (Fig. 11). SV2 observed several small "eddies/ rolls" in the low-level inflow tail that appeared as small horizontal vorticity "rolls", within the tail cloud flowing toward the southwest from the front-flank cold-pool area towards and into the rotating updraft base (Fig. 12).

Figure 11: SV2 GPS location at 2056:10 UTC (Stanton, NE, and Pilger, NE, highlighted in red). Base image by Google Maps.

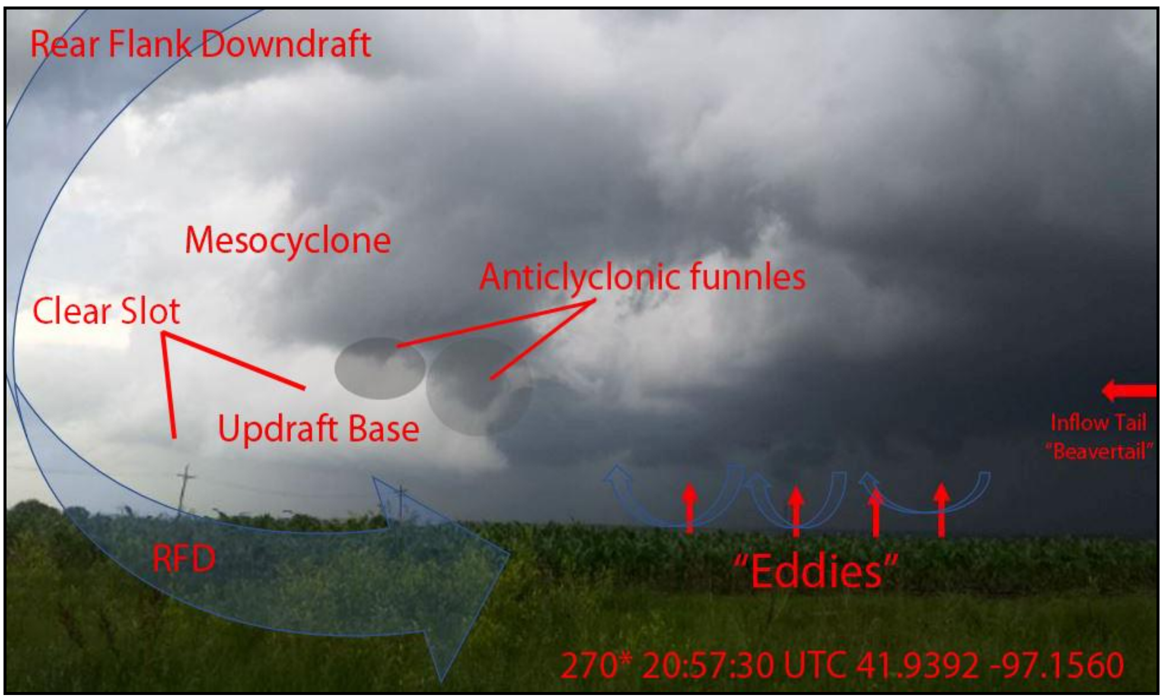

Figure 12: SV2 photo of the low-level eddies and associated storm features at 2057:30 UTC. Picture by L. Dean.

These eddies would curl quickly down and then back up into the inflow tail cloud to the north of the updraft-downdraft interface (hereafter UDI) area. From 2056:10 through 2057:30 UTC, these features were present visually and were documented by SV2. Additionally, a rear-flank downdraft (hereafter RFD) clear slot was observed (Fig. 12), where the eddy features appeared to weaken near the UDI area. Two small anticyclonic funnels were also observed near the leading edge of the RFD (Fig. 12). SV2 relocated to the east at 2057:40 UTC to avoid a possible RFD wind surge and the anticyclonic funnels.

Orf et al. (2017, hereafter O17) theorized that the location of or very near the eddies, like those seen in Fig. 12, is part of a region of streamwise vorticity current (hereafter SVC). Model simulations, as in O17, suggest that these features may have significance regarding tornadogenesis. The simulations in O17 prior to tornadogenesis showcase both anticyclonic and cyclonic rotation as the SVC is tilted upward into the updraft (their Figs. 6 and 7). Visual observations from SV2 and SV1 seem to support the O17 simulations in both time and location.

At 2109:54 UTC, SV1 visually observed the Pilger west tornadogenesis (from his viewpoint) and associated RFD clear slot from 835th Ave. (41.9309N –97.1001W), some 12 min after SV2 observed the eddies and anticyclonic funnels (Fig. 13).

Figure 13: Video screen capture from SV1 of the Pilger, NE west tornado and RFD clear slot at 2109:54 UTC. Red lines denote clear slot. View toward west-northwest. Courtesy C. Rice.

Observations from SV1 highlight some interesting features within the forward-flank downdraft boundary (hereafter FFDB) inflow tail region. At 2110 UTC, the FFDB cloud region was not visually as low in height above ground level as the previous SV2 observations, appearing as a smooth, laminar base angled southwest towards the UDI area (Fig. 13). Also, at the intersection of the UDI and FFDB areas, condensation became visible with scud clouds forming and being pulled into the UDI area, while the FFDB appeared to accelerate into the UDI area or possibly the low-level mesocyclone or even the tornado itself.

Ultra-high-resolution simulations of a long-track tornado, as highlighted in O17 and Orf et al. (2018, hereafter O18), suggest that the FFDB cloud height difference noted in time between SV1 and SV2 visual observations may be a product of the SVC being tilted vertically into low-level mesocyclone. This may explain the change in height of the inflow tail cloud and the transition of the inflow eddies to a laminar inflow cloud base, as highlighted in O17 (their Figs. 10 and 11), along with our visual observations.

SV1 and SV2 locations at 2109:56 through 2112:50 UTC were south and southeast of the

DT probe deployment location and tornado. Video observations from SV1, SV2, and DT confirmed that the northeastward-moving Pilger west tornado increased in size just after the probe had been deployed and activated (next section).

On radar (Fig. 14), a large tornado debris signature (TDS) with low correlation coefficient values was evident by 2109:56 UTC, very near the DT location.

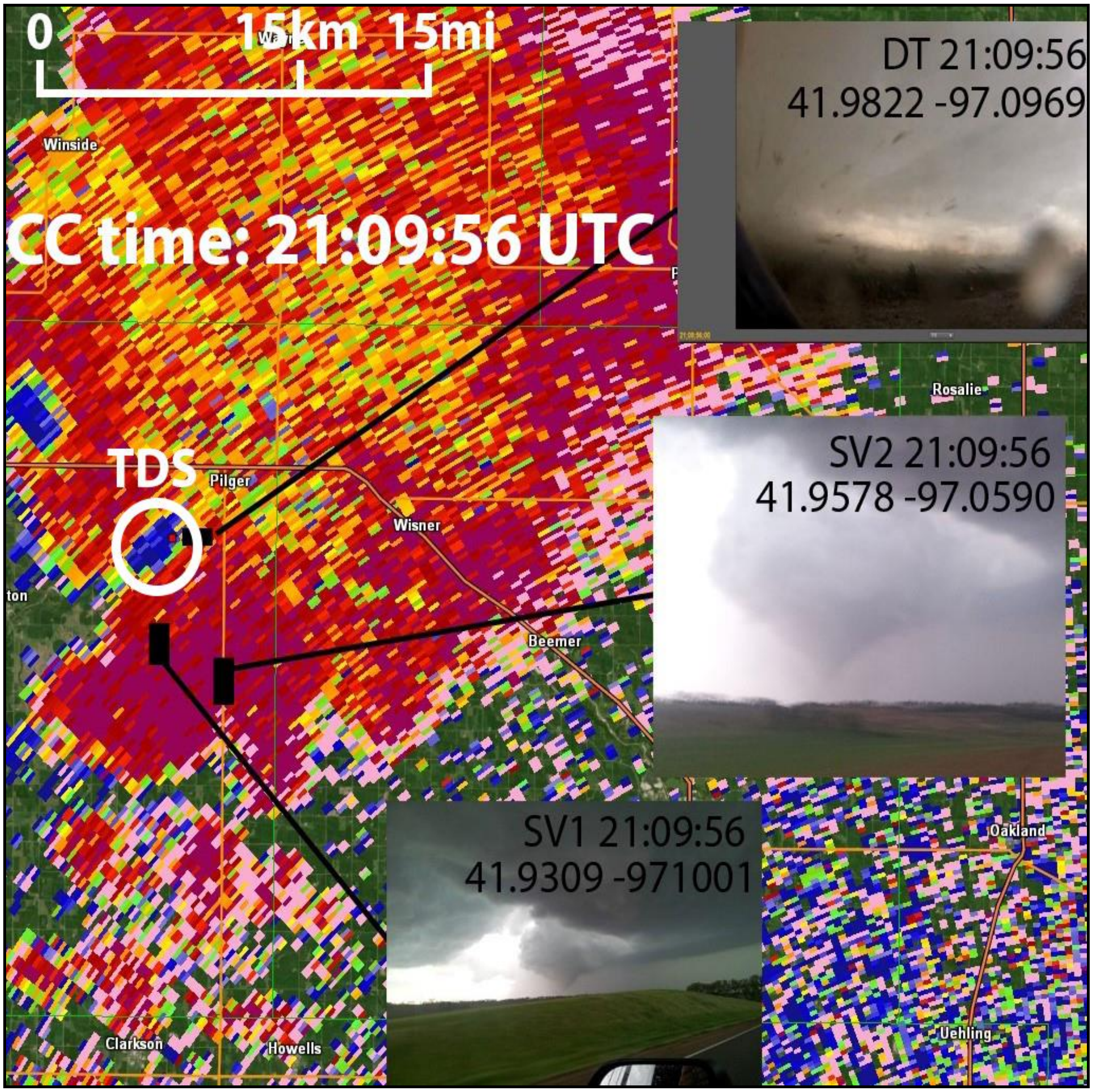

Figure 14: NWS Omaha/Valley, NE (KOAX) 0.5°-elevation cross-correlation coefficient product at 2109:56 UTC with GPS locations (black rectangles) of SV1, SV2, and DT (inset images). Tornado debris signature (TDS) highlighted and circled in white.

5. Probe-based observations

At 2108:57 UTC, PACRITEX DT deployed a ground-based video probe roughly three miles southwest of Pilger, NE, near the junction of 838 1/2 Rd and 572nd Ave. The deployment location (41.98227N –97.09696W), just west of the Pilger Sand and Gravel Pit (Fig. 15), offered an unobstructed view of the oncoming Pilger west forming tornado. Probe video (Fig. 16 Pilger probe video 1) shows that the Pilger west tornado had just developed and was to the southwest of the probe, moving northeastward in a vortex-breakdown state (Trapp 2000).

Elapsed time of probe deployment to the start of impact (hereafter SOI) of the Pilger west tornado was 51 s. Video and photogrammetry analysis (Rasmussen et al. 2003; Holle 1982) revealed calculated winds sustained at roughly 29 m s^{-1}, 15 s after deployment at 2109:10 UTC in association with a strong easterly inflow jet. At 2109:46 UTC, probe video analysis and photogrammetry calculations further reflect an increase in wind speed to roughly 54 m s^{-1}. This was the SOI to the PACRITEX video probe (Fig. 17). The temporally averaged wind speeds from 2108:57 through 2109:46 UTC, as highlighted in Fig. 17, were derived by a variation of calculations from three photogrammetric methods, which included

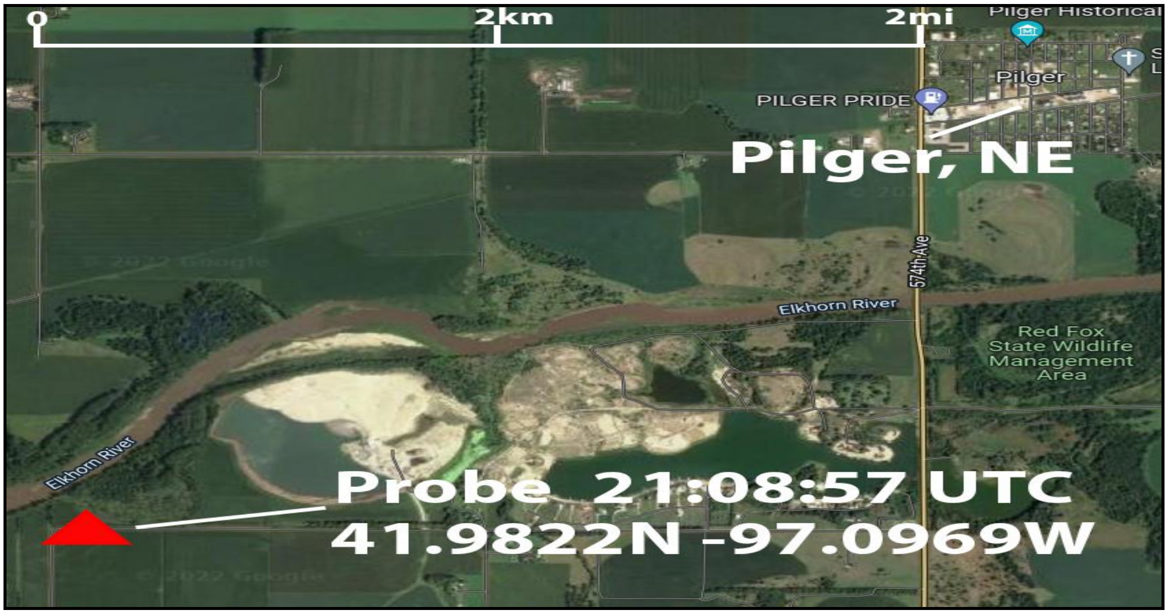

Figure 15: Probe deployment location (red triangle) with GPS and time. Pilger, NE location upper right highlighted in white. Background image courtesy Google.

Figure 16: Pilger Probe video 1 pre, during, and post-impact. Probe view looking west. *Click link to play and enlarge.*

(i) manual calculation (Saunders 1963; Holle 1982), (ii) automated (Rasmussen et al. 2003), and (iii) software calculations. The results of the Pilger west photogrammetric analysis and detailed calculations will be highlighted in a future publication. A history of photogrammetric methods and techniques are cited amply elsewhere (Forbes and Bluestein 2001; Bluestein and Golden 1993; Golden and Purcell 1977; Holle 1982; Slama 1980).

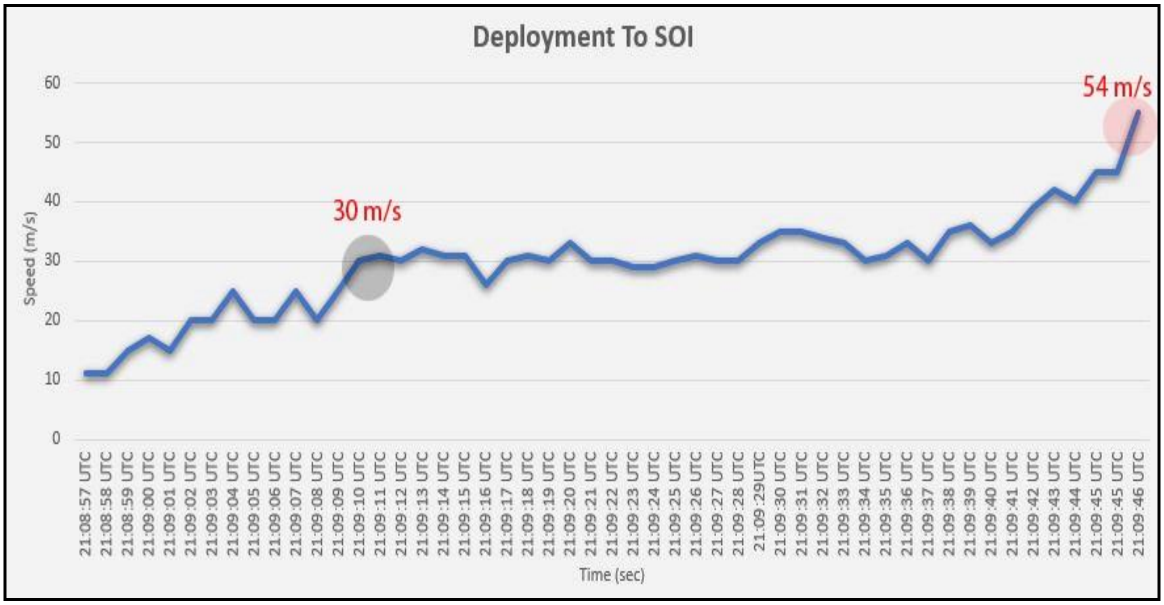

Figure 17: Time and wind speed at 1-s intervals. Deployment of the probe to start of impact (SOI) 51 s.

a. Visual and time scale of subvortices

Probe-based video observations of the Pilger west tornado spotlight the complexities of a large multiple vortex tornado that continues in a state of breakdown for a considerable length of time (i.e., the entire documented probe deployment timeline). From the time of deployment of the probe at 2108:57 UTC, multiple subvortices can be seen evolving and dissolving on the order of seconds or fractions of seconds, while rotating about a concentric axis point that was not always clearly visible or well defined. Before, during, and after the SOI to the video probe, video analysis, and DT observations reveal fascinating morphology within the interior tornado core. In Fig. 18a (Pilger probe video 2a), nine subvortices and mini subvortices are present, but appear to dissipate rapidly, transitioning into three larger subvortices (Fig. 18b). Video analysis of probe video 2b shows the transition of these mini subvortices into separate larger subvortices occurred from 2109:35 UTC to 2109:36 UTC, a period of 2 s or less. Moreover, transitions from mini subvortices to larger subvortices continue repetitively through the entire span of the video probe documentation, during the Pilger west tornado.

Although the authors are confident in the results of their findings and the total subvortices count, a reasonable argument could be made that some of the vortices seen in Fig. 18a are possibly different sides of singular vortices that are close together. This is attributed to a skewed video viewpoint of the multiple vortices from the video probe. Because the film plane is not three-dimensional in nature, and because the vortices identified in Figs. 18a–b are highlighted two-dimensionally via a simple line (x,y), one might see how the lack of depth of the pixeled videographic frames skew the viewpoint of the respective vortices from the probe wide-angle camera lens. Figure 19 shows the viewpoint from the probe with the estimated location and distance of some of the individual vortices at 2109:35 UTC.

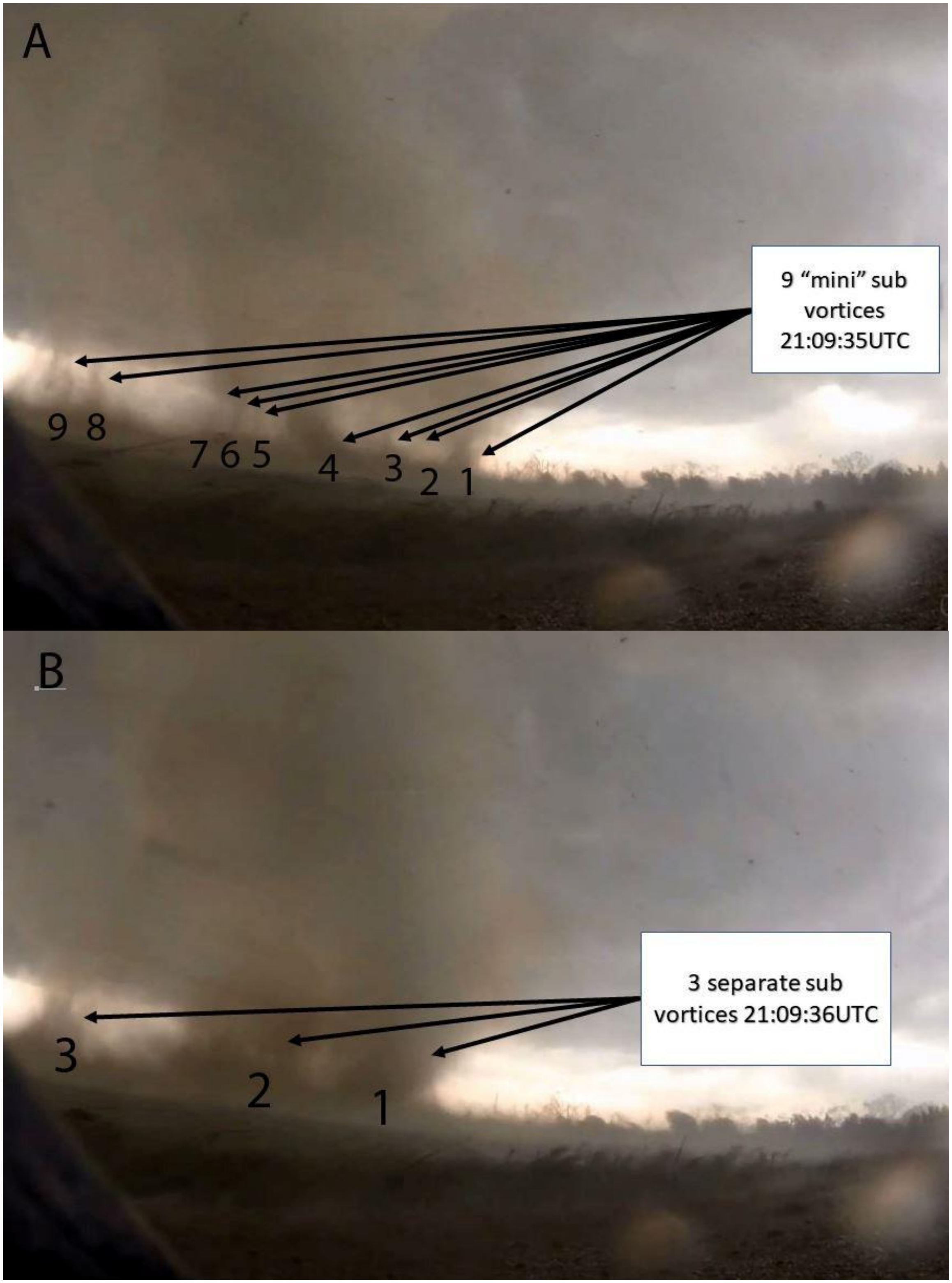

Figure 18: Pilger probe video 2a and probe video 2b: a) Nine mini subvortices transitioning to b) separate, larger subvortices. *Click links to play and enlarge.*

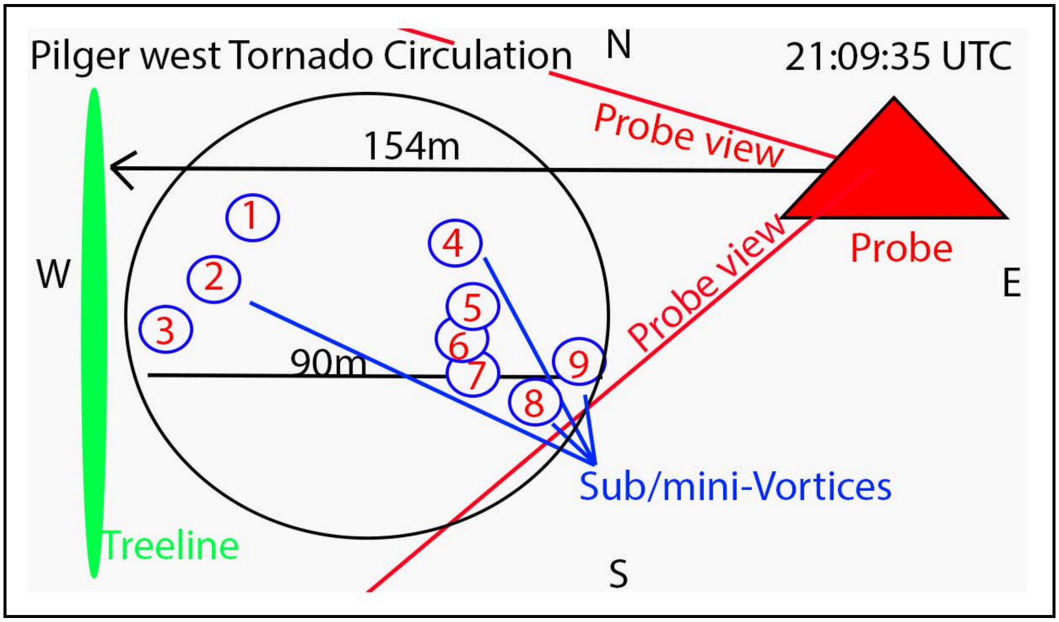

Figure 19: Pilger west estimated sub/mini-vortices location at 2109:35 UTC, with probe and tree line locations.

This skewed viewpoint, due in part to the wide-angle camera lens, and the two-dimensional plane line in Figs. 18a and 18b, is further exposed when comparing the distances between the various subvortices. For example, the measured distance from the video probe to the tree line west of 572nd Ave. was 154 m. The estimated distance between vortex #3 and vortex #9 was nearly 90 m (Fig. 19). Similarly, vortices #5, #6, and #7 might appear to be behind and to the south of vortex #4; however, detailed video analysis shows these vortices to be immediately south of vortex #4 and nearly vertically even with it, as they traverse towards vortex #4, ultimately merging into one large subvortex (Fig. 18b, subvortex #2). This distance and position of the vortices are not represented well in Fig. 18 due to the aforementioned skewed video issues. Additionally, the vortices presented in Fig. 18a can only be described as "mini" vortices as each parent subvortex appeared to enter a vortex breakdown phase within an already existing breakdown phase (mini vortices within the subvortex). The authors feel confident in the total number of vortices identified in Fig. 18a and the general estimated location of each respective vortex.

Prior to this project and this video from the Pilger in-situ tornado probe, the authors are not aware of any video data that have been collected to document such rapid subvortex transitions. This raises questions about how subvortices transition so rapidly, as seen in the Pilger probe video, and how subvortices within a tornado that is already in a breakdown state dissipate and break down further. Answering such complex questions is certainly beyond the scope of this paper. But the visual record here does appear to confirm that such changes do occur, and they can occur very rapidly, on the order of seconds or even fractions of seconds.

Field research from Wurman and Kosiba (2013, hereafter WK13) delineate this rapid secondary vortex breakdown phase feature as "Higher-order multiple vortices" (e.g., multiple vortices within multiple vortices; their Figs. 13c,d) that are within or part of the multiple vortex mesocyclone (MVMC). W14 further emphasizes these vortices as "interior vortices" which are likely described by Seimon et al. (2016, hereafter S16), as observed and recorded by a third party roughly 0.5-km from the 31 May 2013 El Reno, OK EF3 tornado (the S16 third-party documentation correlates well with the WK13 and the W14 formal literature). In similar fashion, additional videographic observations from the PACRITEX DT located a few hundred meters to the east of the Pilger west tornado and probe location documented at least four large subvortices (Fig. 20 Pilger DT video), containing several sub-scale "mini" vortices (internal vortices within subvortices).

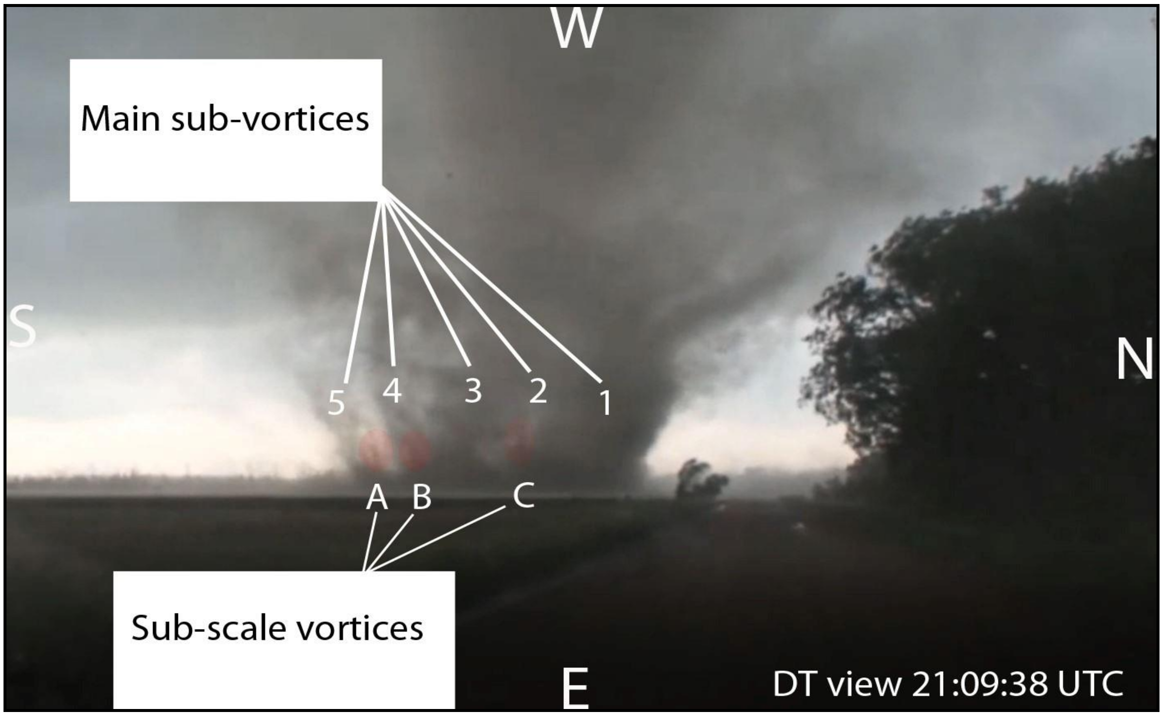

Figure 21: Video screen capture of deployment team video (Pilger DT video) showing main subvortices and "mini sub-scale vortices". Video screen capture by R. Hicks. *Click link to play and enlarge.*

The authors believe that the PACRITEX in-situ video observations of the 16 June 2014 Pilger, NE west tornado may be the first in-situ video documentation that visually showcases the WK13 "Higher-order multiple vortices" (breakdown phase within a breakdown phase), and the S16 published literature. We are unaware of any other in-situ documentation where nine subvortices were visually documented concurrently and where such rapid subvortex transitions were observed and recorded.

b. A single independent vortex

Figure 21a–d (Pilger probe video 3), highlights probe video from the top probe camera only and reveals an in-depth look into the low-level mesocyclone/tornado core from the upward-facing probe camera. Particular interest from the upward-facing probe camera comes during the 2109:57–2110:03 UTC timeframe, as a long cylinder vortex can be seen revolving on the outside of the parent tornado. This vortex was cyclonic and curved outward and away from the parent tornado core, but was connected to the outer rim region of the upper section of the low-level mesocyclone. Although this vortex did not produce full visible condensation extending to the ground from the probe viewpoint, damage and lofted debris are seen from the southwest-facing probe camera, roughly 60–90 m west of the visible tornadic condensation circulation at 2110:01–2110:03 UTC (Fig. 22 Pilger probe video 4). No similar independent vortex feature was visible throughout the remainder of the entire video probe documentation.

The lofted debris noted to the west of the probe in Fig. 22 and the Pilger probe video 4 may have been caused by a rear inflow jet or the rear-flank downdraft. Wakimoto et al. (2015) described lofted debris/dust near a tornado's periphery, possibly owing to tornadic winds from the parent circulation or the RFD, such as during the 31 May 2013 El Reno, OK EF3 tornado. Because little condensation is seen from the westerly-facing probe camera during the 2110:01–2110:03 UTC timeframe, and because a strong northerly wind is seen lofting debris in a southerly direction and causing damage at nearly the same time, one could argue that the single independent vortex had already been ingested into the parent vortex, and the damage noted in Pilger probe video 4 (Fig. 22) was caused by an inflow jet or RFD. From the Pilger probe video 4, this seems a possible scenario as the independent vortex was moving in a quasi-cycloidal path from 2109:57–2110:01 UTC, on the northern side of the tornado core, where it appeared to be very close to being ingested into the parent vortex, as it moved northerly and then westerly. Nevertheless, was this single independent vortex a satellite tornado (Edwards 2014, hereafter E14), a suction vortex (Fujita 1971), or an orbiting subvortex (Fujita and Forbes 1976)?

Figure 21: Upward-facing probe video captures of a separate, single vortex outside of the Pilger west parent tornado at a) 2109:57 UTC, b) 2109:58 UTC, c) 2110:00 UTC, and d) 2110:01 UTC (Pilger probe video 3). *Click link to play and enlarge.*

Figure 22: Video screen capture of Pilger probe video 4 showing lofted debris and damage outside of the visible condensation circulation 2110:03 UTC. *Click link to play and enlarge.*

E14 suggested segregation of satellite tornadoes from main tornadoes and other vortices such as subvortices and interior vortices (e.g., WK13), and defined a satellite tornado as a discrete, closed vortex, occurring "adjacent to a larger and or longer-lived mesocyclone", but acknowledged the obvious difficulties in discerning various types of vortices within, or close to, the mesocyclone. Edwards and Dean (2018, hereafter ED18) continued attempts at explicitly segregating satellite tornadoes by observational examples but did not include a dynamic definition or a descriptive distance spatially. While there are many published findings describing phenomena such as subvortices and suction vortices (Ward 1972; Rotunno 1977, 1979; Fiedler 1993), little formal literature exists quantifying the difference between satellite tornadoes and subvortices or multiple vortices spatially (Aydelott 2021, personal communication).

A three-class scale for multiple vortices was proposed by Potts and Agee (2002), which defined a ten-tier vortex sub-scale classification, but lacked quantification of spatial distance in classifying such vortices. Fujita et al. (1970), and Bluestein et al. (2018), both referenced a rough spatial scale of 1–10 m as the sub-tornado scale, but if the damage highlighted during the 2110:01–2110:03 UTC timeframe was caused by the Pilger west single independent vortex (Fig. 21), it does not fall within the sub-tornado scale. Laboratory models and numerical simulations of subvortices, near or within multiple vortex tornadoes, show that they can lean outward radially with height in the direction of the azimuthal flow (Rotunno 1984), but are a part of, or attached to, the parent tornado circulation (Bluestein et al. 2015), similar to Fig. 21a–d, and as seen in Pilger probe video 3.

Research from Doppler on Wheels (hereafter DOW) beginning in 1995 (see WK13) probed some 170+ distinct vortices and dynamically categorized those vortices associated with supercell thunderstorms. WK13 suggested that multiple vortices within broad mesocyclones can readily change state from single vortex tornadoes to multiple surface circulations and then back to a single vortex state. WK13 further concluded that there was no clear spatial-scale separation between multiple vortex circulations, large multivortex tornadoes, or even some sub-scale type vortices.

Since WK13 did not describe or include a spatial scale of satellite tornadoes, and did not acknowledge satellite tornadoes as independent vortices in their findings, but rather lumped these types of vortices into a broader class of the MVMC, one has to consider that a single independent vortex like that documented with the Pilger west tornado was a satellite tornado. It does meet most, if not all, of the requirements of a satellite tornado as defined in both E14 and ED18, in that the parent storm was a supercell, the vortex was a discrete and closed vortex, and appeared to be immediately at the edge of a larger long-lived main tornado (MT), translating around it, and likely ingested/merged into the parent vortex, similar to E14 Fig. 1. However, according to the top view probe camera FOV (Fig. 21), the single independent vortex also appeared to originate from the upper rim of the low-level mesocyclone/tornado core and possibly within it, which raises questions about categorizing it as a satellite tornado.

From an additional six-tier scale discussed in Agee et al. (1976) and the aforementioned WK13 classifications, this vortex might also be considered an independent orbiting subvortex (IOSV), very near the main tornado at ground level, yet also within the tornado circulation at cloud base, similar to the WK 13 "widened coil tip" vortex. The Pilger west independent vortex seems to meet both E14/ED18 and WK13 conceptual models, leaving the authors uncertain in dynamically categorizing this vortex herein.

At any rate, the authors are unaware of any previous formal in-situ video research successfully documenting the tornado core from an upward-facing video camera. Moreover, the authors believe this is the first time that an upward, in-depth look into the lower-level mesocyclone/tornado core has been achieved, revealing an independent vortex or satellite tornado in such proximity to the parent circulation, and is a first-ever observation.

6. Future work

A full photogrammetric analysis of the Pilger, NE west tornado has been completed and will be used to complement this study in a future publication. Previous successful PACRITEX probe deployments near and in situ have been obtained during the 30 March 2016 Tulsa, OK EF2 tornado, 25 May 2016 Chapman, KS EF4 tornado, 16 May 2017 Elk City, OK EF2 tornado, 23 February 2018 Burnsville, MS EF2 tornado, and the 24 May 2021 Seldon, KS EF1 tornado. These infrasonic, video and pressure-deficit data sets will also be presented in future publications.

7. Summary and discussion

On 16 June 2014, a privately funded research campaign successfully placed a ground-based in-situ video probe in the direct path of the Pilger, NE EF4 west tornado. The video probe was equipped with three video cameras, which documented unique and important observations not previously documented within existing in-situ research. Video inferred from the probe shows that it was impacted by the left-front quadrant of the tornado core approximately 51 sec after activation and deployment. The video probe did not loft or slide and successfully survived the harsh tornadic winds. Video analysis shows that the Pilger west tornado was in a continuous vortex breakdown state during the entire probe documentation, and probe visual observations resolved fine details of the tornado core, which included as many as nine subvortices at one point, with multiple sub-scale vortices (interior vortices). This documentation is likely the first in-situ visual observation of the "Higher-order multiple vortices" as outlined in WK13 and S16.

The upward-facing video probe camera documented a single independent vortex revolving around the Pilger west tornado core. This independent vortex curved outward and away from the parent multiple vortex core but was attached to the upper rim of the low-level mesocyclone. Video from the upward-facing probe camera highlights the independent vortex tracking in a quasi-cycloidal path from 2109:57 through 2110:01 UTC on the northern side of the tornado core/hook echo. Synced video from the westerly facing probe camera shows lofted rotating debris from 2110:01 through 2110:03 UTC, roughly 60–90 m to the west of the Pilger west tornado core as the independent vortex traversed northwesterly, to westerly, out of the FOV of the upward-facing probe camera. The single independent vortex may already have been ingested in the Pilger west parent vortex before the lofted debris is seen to the west of the probe with the lofted debris caused by an inflow jet or the rear flank downdraft. The authors concede that this is a likely scenario, although not certain.

The time span of the near half revolution of this single independent vortex, as seen from the upward-facing probe camera to the documented rotating lofted debris from the southwest-facing probe camera, was just over four seconds. E14 and ED18 define the Pilger west independent vortex as a satellite tornado, and the vortex does meet all the E14 and ED18 satellite tornado requirements. However, this independent vortex also shares some of the WK13 attributes as an orbiting subvortex, most particularly the WK13 documented "widened coil tip" vortex. Despite any scientific naming contention, the authors are not aware of any previous formal in-situ video observations of an independent vortex from an upward-facing video probe camera and believe this is likely a first-ever observation.

Additionally, SV2 visual observations of the twin anticyclonic funnels and RFD location prior to the Pilger west tornadogenesis correlates well with the O17, and O18 published literature in time and location. The O17 and O18 simulations may be reflected in the probe and DT observations of the multiple vortices. However, continued field research is needed to validate these possible SVC features and locations, particularly near the FFDB and UDI areas during the genesis and maintenance of the tornado. Moreover, the importance of observations, including video documentation near the afore-mentioned boundaries, is needed to help understand any possible relationship between the low-level SVC and tornadogenesis, as displayed in the O17 and O18 simulations.

While this study does not expound on swirl ratio, corner flow, or axisymmetric wind flow (e.g., Lewellen et al. 1997; Lewellen et al. 2000; Kosiba and Wurman 2010) but instead highlights the in-situ video observations of the Pilger, NE west tornado, the questions, and discussion above are given with the understanding that future in-situ observations and research are still needed to account for, and understand tornadic vortex behavior. The authors hope that the visual documentation of subvortex behavior here will provide continued motivation for additional work and research.

ACKNOWLEDGEMENTS

The authors wish to greatly acknowledge friend, and colleague, the late Tim Samaras. Without his passion and guidance, this paper would not be possible. The authors would like to thank and extend deep appreciation to Jon Davies, who gave valuable insight, time, and constructive criticism, but always continued with words of encouragement. The authors personally thank Roger and Elke Edwards for their time and patience, Rich Thompson for going out of his way to answer personal messages and questions, Dr. Athena Nagel and Greg Nordstrom from Mississippi State University Department of Geoscience, Chris Rice, Kendra Reed, James Aydelott, Lisa McGeough, Roger Hill, Shawna Davies, and Patt Winn, all of whom gave valuable personal time or aided in the research herein. Finally, the authors would like to sincerely thank reviewers Corey Mead and Sean Waugh for their valuable insights and suggestions that improved earlier versions of this manuscript.

Appendix

Video Links:

Pilger probe video 1
https://youtu.be/nBYAaLK-M48

Pilger probe video 2a
https://youtu.be/Y1UHUTIeNew

Pilger probe video 2b
https://youtu.be/3jMrKxk-5ZA

Pilger probe video 3
https://youtu.be/lq6jzhFOmoM

Pilger probe video 4
https://youtu.be/lMB0zmj-3yY

Pilger DT video
https://youtu.be/_mMs6giPnkU

Pilger probe video all three cameras
https://youtu.be/2EyI_oalAHU

Contact Lanny Dean for data availability at led42@msstate.edu.

REFERENCES

Agee, E. M., J. T. Snow, and P. R. Clare, 1976: Multiple vortex features in the tornado cyclone and the occurrence of tornado families. *Mon. Wea. Rev.*, **104**, 552–563.

Bedard, A. J., 2005: Low-frequency atmospheric acoustic energy associated with vortices produced by thunderstorms. *Mon. Wea. Rev.*, **133**, 241–263.

Blair, S. F., D. R. Deroche, and A. E. Pietrycha., 2008: In situ observations of the 21 April 2007 Tulia, Texas tornado. *Electronic J. Severe Storms Meteor.*, **3** (3), 1–27.

Bluestein, H. B., and J. H. Golden, 1993: A review of tornado observations. The Tornado: Its Structure, Dynamics, Prediction and Hazards, *Geophys. Monogr*., No. 79, Amer. Geophys. Union, 319–352.

——, Snyder, J. C., and J. B. Houser, 2015: A Multiscale overview of the El Reno, Oklahoma, tornadic supercell of 31 May 2013. *Wea. Forecasting*, **30**, 525–552.

——, Thiem, K. J., Snyder, J. C., and J. B. Houser, 2018: The multiple-vortex structure of the El Reno, Oklahoma, tornado on 31 May 2013. *Mon. Wea. Rev.*, **146**, 2483–2502.

Edwards, R., 2014: Characteristics of supercellular satellite tornadoes. Proc., *27th Conf. on Severe Local Storms*, Madison, WI, Amer. Meteor. Soc., 17.5.

——, and A. R., Dean, 2018: Environments of supercellular satellite tornadoes. Proc., *29th Conf. on Severe Local Storms*, Stowe, VT, Amer. Meteor. Soc., 51.

Fiedler, B. H., 1993: Numerical simulations of axisymmetric tornadogenesis in forced convection. The Tornado: Its Structure, Dynamics, Predication, and Hazards. *Geophys. Monogr.*, Vol. 79, Amer. Geophys. Union, 41–48.

Forbes, G. S., and H. B. Bluestein, 2001: Tornadoes, tornadic thunderstorms, and photogrammetry: A review of the contributions by T. T. Fujita, *Bull. Amer. Meteor. Soc.*, **82**, 73–96.

Fujita, T, T., 1971: Proposed mechanism of suction spots accompanied by tornadoes. Preprints, *7th Conf. on Severe Local Storms*, Kansas City, MO, Amer. Meteor. Soc., 208–213.

——, and G. S. Forbes, 1976: Definition of suction vortices. Proc., *Symp. on Tornadoes*, Lubbock, TX, Texas Tech University, 79.

——, D. L. Bradbury, and C. F. Van Thullenar, 1970: Palm Sunday tornadoes of April 11, 1965. *Mon. Wea. Rev.*, **98**, 29–69.

Golden, J. H., and D. Purcell, 1977: Photogrammetric velocities of the Great Bend, Kansas tornado of 30 August 1974: Accelerations and asymmetries. *Mon. Wea. Rev*., **105**, 485–492.

Holle, R. L., 1982: Photogrammetry of Thunderstorms: A Social and Technological Documentary, E. Kessler, Ed., University of Oklahoma Press, 77–98.

Karstens, C. D., T. M. Samaras, A. Laubach, B. D. Lee, C. A. Finley, W. A. Gallus Jr., and F. L. Haan., 2008: TWISTEX 2008: In situ and mobile mesonet observations of tornadoes. Preprints, *24th Conf. on Severe Local Storms*, Savannah, GA, Amer. Meteor. Soc., P3.11.

——, ——, B. D. Lee, W. A. Gallus Jr., and C. A. Finley, 2010: Near-ground pressure and wind measurements in tornadoes. *Mon. Wea. Rev.*, **138**, 2570–2588.

Kosiba, K. A., and J. Wurman, 2010: The three-dimensional axisymmetric wind field structure of the Spencer, South Dakota, 1998 Tornado. *J. Atmos. Sci*, **67**, 3074–3083.

——, and ——, 2013: The three-dimensional structure and evolution of a tornado boundary layer. *Wea. Forecasting*, **28**, 1552–1561.

——, and ——, 2016: The TWIRL Tornado Winds from In-Situ and Radars at Low-Level project. Proc., *28th Conf. on Severe Local Storms*, Portland, OR, Amer. Meteor. Soc., 15.3.

Lee, J., T. M. Samaras, and C. Young, 2004: Pressure measurements at the ground in an F4 tornado. Preprints, *22nd Conf. on Severe Local Storms*, Hyannis, MA, Amer. Meteor. Soc., 15.3.

Lee, B. D., C. A. Finley, and T. M. Samaras, 2011: Surface analysis near and within the Tipton, Kansas, Tornado on 29 May 2008. *Mon. Wea. Rev.*, **139**, 370–386.

Lewellen, W. S., D. C. Lewellen, and R. I. Sykes, 1997: Large-eddy simulation of a tornado's interaction with the surface. *J. Atmos. Sci.*, **54**, 581–605.

Lewellen, D. C., W. S. Lewellen, and J. Xia, 2000: the influence of a local swirl ratio on tornado intensification near the surface. *J. Atmos. Sci*, **57**, 527–544.

Orf, L. G., R. B. Wilhelmson, B. D. Lee, C. A. Finley, and A. L. Houston, 2017: Evolution of a long-track violent tornado within a simulated supercell. *Bull. Amer. Meteor. Soc*., **98**, 45–68.

——, A. Dixon, and K. T. Halbert, 2018: The role of the streamwise vorticity current in tornado genesis and maintenance. Proc., *29th Conf. on Severe Local Storms*, Stowe, VT, Amer. Meteor. Soc., 1.4.

Potts, S. L., and E. M. Agee, 2002: Three scales for multiple vortices. Preprints, *21st Conf. on Severe Local Storms*, San Antonio, TX, Amer. Meteor. Soc., 527–530.

Rasmussen, E. N., J. M. Straka, R. P Davies-Jones, C. A. Doswell III, F. H. Carr, M. D. Eilts, and D. R. MacGorman, 1994: Verification of the Origins of Rotation in Tornadoes Experiment: VORTEX. *Bull. Amer. Meteor. Soc*, **75**, 995–1006.

——, R. P. Davies-Jones, and R. L. Holle, 2003: Terrestrial photogrammetry of weather images acquired in uncontrolled circumstances, *J. Atmos. Oceanic Technol*, **20**, 1790–1803.

Rotunno, R., 1977: Numerical simulation of a laboratory vortex. *J. Atmos. Sci.*, **34**, 1942–1956.

——, 1979: A study in tornado-like vortex dynamics. *J. Atmos. Sci.*, **36**, 140–155.

——, 1984: an investigation of a three-dimensional asymmetric vortex. *J. Atmos. Sci*, **41**, 283–298.

Samaras, T. M., 2006: Dynamic measurements of the lowest 10 meters of tornadoes. Preprnts, *23rd Conf. on Severe Local Storms*, St. Louis, MO, Amer. Meteor. Soc., 14.3.

——, and J. J. Lee, 2003: Pressure measurements within a large tornado. Preprints, *8th Symp. on Integrated Observing and Assimilation Systems for Atmosphere, Oceans, and Land Surface*, Seattle, WA, Amer. Meteor. Soc., 4.9.

Saunders, P. M., 1963: Simple sky photogrammetry. *Weather*, **18**, 8–11.

Seimon, A., J. T. Allen, T. Seimon, S. J. Talbot, and D. K. Hoadley, 2016: Crowdsourcing the El Reno 2013 tornado: A new approach for collation and display of storm chaser imagery for scientific applications. *Bull. Amer. Meteor. Soc*, **97**, 2069–2084.

Slama, C., Ed., 1980: Manual of Photogrammetry. 4th ed. *American Society of Photogrammetry*, 1056 pp.

Thompson, R. L., C. M. Mead, and R. Edwards, 2007: Effective storm-relative helicity and bulk shear in supercell thunderstorm environments, *Wea. Forecasting*, **22**, 102–115.

Trapp, R. J., 2000: A clarification of vortex breakdown and tornadogenesis. *Mon. Wea. Rev.*, **128**, 888–895.

Wakimoto, R. M., N. T. Atkins, K. M. Butler, H. B. Bluestein, K. Thiem, J. Snyder, and J. B. Houser, 2015: Photogrammetric analysis of the 2013 El Reno tornado combined with mobile X-band polarimetric radar data, *Mon. Wea. Rev.*, **143**, 2657–2683.

Ward, N. B., 1972: The exploration of certain features of tornado dynamics using a laboratory model, *J. Atmos. Sci*., **29**, 1194–1204.

Wurman, J., and K. Kosiba, 2013: Finescale radar observations of tornado and mesocyclone structures. *Wea. Forecasting*, **28**, 1157–1174.

——, ——, and P. Robinson, 2013: In situ, Doppler radar, and video observations of the interior structure of a tornado and the wind–damage relationship. *Bull. Amer. Meteor. Soc*., **94**, 835–846.

——, ——, ——, and T. P. Marshall, 2014: The role of multiple vortex tornado structure in causing storm researcher fatalities. *Bull. Amer. Meteor. Soc.*, **95**, 31–45.

REVIEWER COMMENTS

[Authors' responses in *blue italics.*]

REVIEWER A (Sean M. Waugh):

Initial Review:

Recommendation: Accept with major revisions.

Overall Comments: Overall the manuscript is well thought out, organized, and fluid. The work presented here is novel and certainly worthy of publication and highlights some important visual observations of both theorized and radar based tornadic behaviors. Documenting these features and behaviors is critical to our conceptual understanding of tornado behavior and breakdown, and ultimately how damage patterns evolve. Observations such as these are rare and are extremely difficult/dangerous to capture, thus the authors have my commendation for doing so. While the manuscript does present useful work and observations, there are a few critical points that I feel need to be addressed prior to acceptance of the manuscript for publication. None of the points/comments I've presented here are overly difficult, but should add value to the manuscript. Looking forward to seeing this manuscript in publication.

Thank you so much for your helpful and insightful review, which we think has led to improvement in our manuscript. We believe we have addressed all or most issues/comments. Specific responses to each of your comments are included below.

Major Comments: PACRITEX, paragraph 1: What is the scientific objective of PACRITEX? It's mentioned that the core mission is to help fill the void of in situ observations following the loss of Tim Samaras, but this doesn't explain the purpose of these observations. Is the goal of PACRITEX just to collect observations, or is there a science question that is attempting to be answered? If memory serves, Tim was documenting pressure perturbations as a way of improving structure designs to better survive tornadic conditions. Is there something similar that PACRITEX is targeting? It would be useful here to expand on the purpose of PACRITEX and what science objectives it is hoping to address. I for one haven't heard of PACRITEX before, so this is a good opportunity to lay out its foundation in published work.

Agreed. I've amended verbiage and lightly expanded on the multifaceted PACRITEX scientific objectives including citation (Bedard 2005) while attempting to stay on the manuscript topic.

PACRITEX, probe design: The probes are using a number of GoPro cameras to record video footage. The authors comment on the sensor of the cameras, as well as the resolution and frame rate setting. It might be worth noting which of the various GoPro versions were used. My experience with GoPros in the past have been that you have very limited control over the internal settings of the video, that the GoPro itself sets things like exposure, focus, DoF, shutter speed, etc. on its own and in real time, often changing settings on the fly during video collection. I've also seen cases where the frame rate fluctuated slightly during collection. Can the authors expand on how potential changes in these settings could affect their observations?

I've added the GoPro camera versions/type (Hero 2) accordingly. While the limited control of features like DOF, shutter speed, etc., is a partially correct statement, the user does have some "wiggle room" to make some changes, with exception of the white balance in some older versions, which would have no effect on video recording capabilities.

*We are a little uncertain on the question of potential changes. If we understand the question correctly, [the reviewer] is asking if we can comment on video changes he has experienced personally, or what one *might* experience if having the types of issues he has experienced, and then apply that to our findings/observations? Even in knowing the reviewers type of media recorded to (SD card), class of card, editing software, ingest process, video resolution, etc.... I do not believe we, nor anyone can answer this question, and in doing so would only be speculative at best on our part. Please accept our apologies if misunderstood.*

Having used most of the various GoPro units available on the market during many years in broadcast media, (original GoPro, Hero 1 through 9), we have personally not experienced the concerns/issues mentioned, most particularly in video mode or with video frame rates. Depending on the software used to encode/decode the video, the user can see the continuous frame rate throughout each entire video clip when/after ingesting. Thus, one can see if there are any issues such as video frame rate upon ingest, prior to completing any editing. Additionally, when placing video clips on the timeline or within the video editing bins, the user can see all video attributes including frame rate, and can validate any possible video fame issues or concerns during the editing process. For example, Adobe Premier Pro or Final Cut Pro allows full view of said frame rates. I've attached a screen capture of the frame rate and location within Adobe PP 2022 for validation below. There were no video frame issues with any of the three GoPro cameras during the 16 June 2014 Pilger west documentation, or issues as described above.

We would be more than happy to discuss the reviewers' cases of frame rate fluctuation and assist in the inner workings of editing software, video recording, and frame rates in an informal setting.

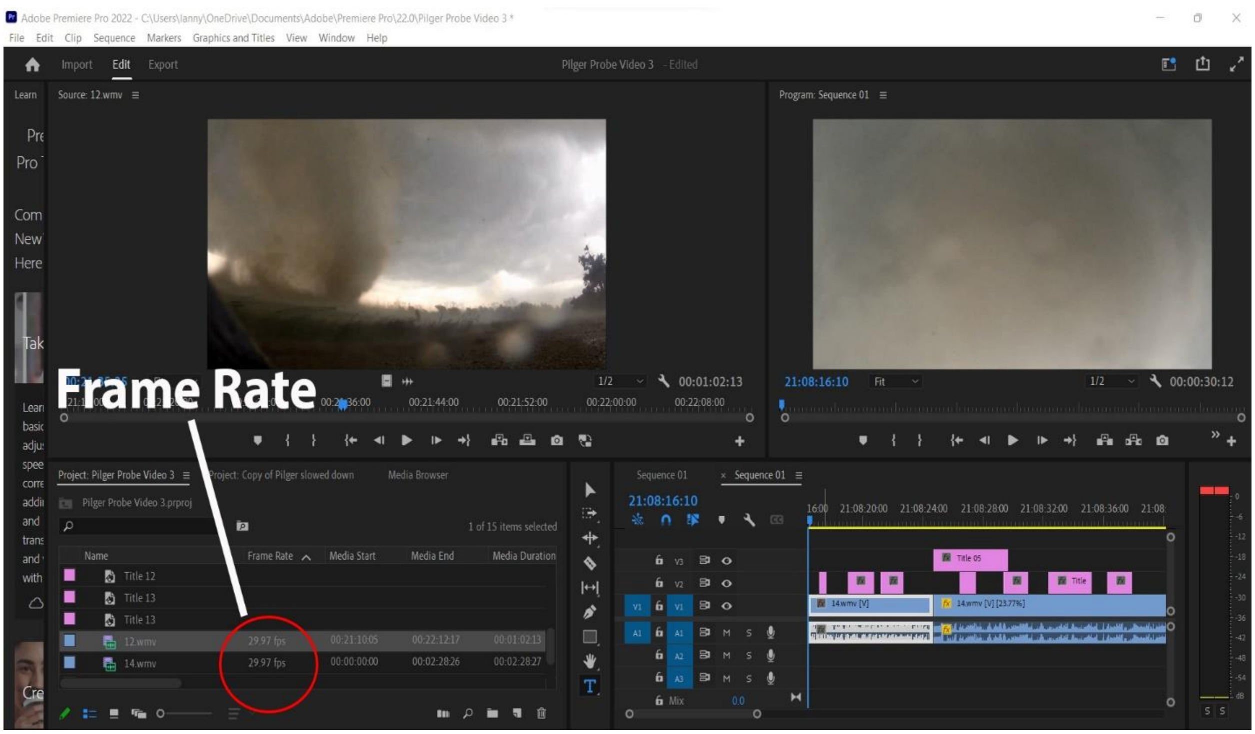

The authors elaborated on the lack of testing of the probe prior to deployment (understandable given the difficulty of testing this, though if the authors would like I have some thoughts on how this could be accomplished), and mention that the first deployment was the Pilger tornado. Can the authors add a bit here as to whether the probe actually moved at all? Given the analysis of video, it is important for the probe to have remained completely stationary during the analysis period, without moving, sliding, or turning, while capturing video. Is there any instrumentation in the probe design to indicate heading or orientation? [Watching the video, the probe doesn't appear to have moved, but a discussion to that point in the manuscript is needed.] Update: I see that this is mentioned in the summary and discussion section, but it should be reiterated here so that the readers understand that the probe did not move during deployment (no small feat by any means).

While both video probes have now survived two violent EF4 tornadoes in situ (Pilger, NE and Chapman, KS), two of our meteorological INPAR (Infrasonic Pressure Acoustic Recorder) probes have also survived two EF2 tornadoes (Tulsa, OK and Burnsville, MS), but we would be more than happy to discuss further testing!

Have amended verbiage to "first successful deployment during PACRITEX campaign…" Our first informal successful in situ video observation was on 29 May 2004 (Conway Springs, KS F-3). The results of that observation were highlighted during our Nat. Geo. special with Tim S. and Sean C. in 2004, and again on "Tornado Hunters" (TuTV in 2007).

I've amended and added to section 3b to include the video probe did not move, slide, turn or loft (some concerns of repetitiveness: section 7). Validated with the video recordings of all three cameras as well as the position of the" FRONT/REAR" facing lettering/logo (Fig. 8). I also changed Fig. 8 to more clearly show the bold lettering ("FRONT/BACK"). The "FRONT/REAR" marking in bold letters is to help orientate the "FRONT" facing camera towards the area of interest at time of deployment, and helps validate any lofting or sliding when retrieving the video probe. Section 7, first paragraph, last sentence, also highlights the video probe did not move, slide or loft and survived the harsh tornadic winds. We believe that we have now clearly communicated (and shown through the video) that the probe did not slide, loft, or turn in section 3b and in section 7.

Probe-based observations, paragraph 3: The estimates of wind speed through video analysis is interesting and unique. While the authors do cite previous work here, given the relatively small amount of literature on this and the importance of these observations to the content of the paper, I would like to see some small discussion on how these calculations are done.

Have added a small section on photogrammetric methods, calculation, and citations for a history of storm photogrammetry. As mentioned, we have cited previous work on photogrammetric analysis for our calculations (Rasmussen et al. 2003; Holle 1982 etc.) in which cosine and fundamental calculations for the automated script can be seen in the latter. As highlighted in Section 6, we have completed a full photogrammetric analysis of the Pilger NE west tornado that will be used to complement this study in a future publication.

We debated any discussion of photogrammetry in this manuscript but chose to lightly introduce parts of the photogrammetric analysis rather than spotlight, so as not to clutter up the focus of the manuscript. We respectfully disagree on the "small amount of literature" on photogrammetry and being "unique." For example, a photogrammetric analysis was completed on the 2 April 1957 Dallas, TX tornado allowing wind flow characteristics and wind speed to be measured (Hoecker 1960). In the 1970s, Ted Fujita used pictures and home movies utilizing photogrammetry to study tornado wind speeds through analyses of the movies of dust/debris clouds and tornadoes or funnel clouds. A quick AMS search will reveal a plethora of additional literature: "Tornadoes, Tornadic Thunderstorms, and Photogrammetry: A Review of the Contributions by T. T. Fujita" (Forbes and Bluestein 2001), "The LaGrange Tornado during VORTEX2. Part II: Photogrammetric Analysis of the Tornado Combined with Dual-Doppler Radar Data" (Atkins et al. 2012), "Photogrammetric Analysis of the 2013 El Reno Tornado Combined with Mobile X-Band Polarimetric Radar Data" (Wakimoto et al. 2015), "The Dodge City Tornadoes on 24 May 2016: Damage Survey, Photogrammetric Analysis Combined with Mobile Polarimetric Radar Data" (Wakimoto et all. 2018), "A Stereo Photogrammetric Technique Applied to Orographic Convection" (Zehnder et al. 2007) just to name a few.

The text referencing Fig. 16 highlights a 29 m s^{-1} and a 54 m s^{-1} gust that were calculated off video analysis, however the figure shows a continuous graph of wind speeds at 1 second intervals. Were these calculations done manually over this entire period or was this automated? What amount of uncertainty is associated with these calculations? It would be helpful to indicate the potential range of velocities on the figure to give readers an estimate of how accurate these calculations are.

"Gusts that were calculated off video analysis" is an incorrect statement. We state: "Video and photogrammetry analysis" for both numerical values. Please see above. Without "giving away" our hopeful future publication, the in-situ photogrammetric calculations of the Pilger west tornado were completed via automated (Rasmussen et al. 2003), manually (Holle 1982; Saunders 1963) and in software throughout the entire in situ observation, but focus was placed on the timeframe listed to the SOI of the video probe for this manuscript. As highlighted and tested in Rasmussen et al. 2003, this automated photogrammetry technique ("Rasmussen "technique") is very accurate and is an extension of the Saunders (1963) manual technique.

While the Pilger photogrammetric calculations do show a potential range of velocities, they are in generally good agreement with the NWS damage rating findings prior to the SOI. However, velocities derived from the Pilger west photogrammetric analysis just after the SOI differ largely from the official NWS damage assessment and subsequent EF rating for the specific location of, and near the video probe (the probe area location). As mentioned, these findings will be highlighted in a future publication.

The initial discussion of the video (referencing Fig. 17) mentions numerous subvortices on extremely short time scales that are difficult to determine from the small video stills. After watching the video repeatedly, there are numerous subvortices present, but it's possible that some of the different subvortices identified in Fig 17a are actually just different sides of singular vortices (they're really close together and given the short time scales these are apparent this introduces some uncertainty). Can the authors comment on the potential that some of the sub vortices identified should possibly be combined? This is more or less asking the authors to comment on the potential uncertainty of their estimate of the number of vortices.

We respectfully strongly disagree regarding combining vortices and total count. However, I've amended Section 5a adding a paragraph addressing this question, noting the skewed video view due to the videographic plane being two-dimensional, and the wide-angle probe camera. I've also added a new figure to highlight the position and general location of the vortices. In Fig. 18a (old Fig. 17a) there are 9 distinct, "closed" vortices present. Per minor comment [editor: omitted], I have increased Figs. 18a,b which we believe now clearly show each respective vortex.

This may ultimately be a minor comment, but given that it's critical to the science presented in the manuscript I felt that it should be in the major section. The links to the videos should be provided explicitly, possibly at the end of the acknowledgements or in line where the hyperlinks are placed. Some users systems may not allow following external links and would need to be typed in manually. For completeness, I would just include the links (they're short too so this shouldn't be a massive issue). Additionally, I'd like to see a statement somewhere regarding data availability. While the videos are on YouTube and accessible through this manuscript, someone may want to work with the raw data themselves. Having a point of contact or location on where the data would be reachable would be helpful to the larger scientific community. Data availability has been a big push in the last several years throughout many of the journals.

I've placed the video links at the end of the Acknowledgments section with data-availability info as requested. Admittedly, we are not familiar with EJSSM policies in allowing video hyperlink placements outside of the body text, please accept our apologies if not appropriately placed.

[Editor comment: They are properly placed; however, we'll probably relabel them as an Appendix in the same spot (below Acknowledgments) if the paper is accepted.]

[Minor comments omitted...]

Second Review:

Recommendation: Accept with minor revision.

[Minor comments omitted...]

REVIEWER B (Corey M. Mead):

Initial Review:

Recommendation: Accept with minor revisions.

General Comment: The manuscript entitled, "In Situ Video Observations and Analysis of the 16 June 2014 Pilger, Nebraska EF4 west Tornado" offers an "up-close" perspective of a violent tornado occurrence. Fine-scale details of such an event are captured by video recordings from a strategically placed probe with those video observations then related to specific features identified in past mobile doppler radar observations and high-resolution model simulations.

I did not review part 3 (PACRITEX), due to my lack of familiarity with sensor fabrication. Nonetheless, I found the paper to be well-organized and novel in approach (i.e., apparently only a handful similar studies have appeared in formal literature) with no glaring fundamental issues. As such, I recommend [to] accept with minor revision. I have submitted my review of the manuscript with the comments/concerns in the margins.

[Editor's Note: Though "minor" revisions were categorized overall, a few of the comments and replies were substantive enough, and contributed strongly positively to the discussion and revisions, to include in the review record.]

Substantive Comments: Fig. 8 in Blair et al. 2008 shows a video capture within the mobile mesonet vehicle immediately after the tornado passage.

Have amended this section to reflect. However, the authors believe the Tulia video observation to be near in situ as the tornado was already some distance from the observers and moving away from them. In situ requirements for this case study required the instrumented video package be in, or come under, direct contact with the interested subject (i.e., the tornado core). Therefore, it is unclear if any intentional in-situ video observations were documented during the Tulia, TX event.

Convergence along/north of the OFB was the primary focus for initiation of the tornadic supercells.

Agreed. Because Corey worked this event, his comments are especially important to this case study. Have restructured to highlight the importance and have included and additional figure (new Fig. 4) to reflect the convergence along and north of the OFB.

I would recommend citing the effective bulk wind difference (EBWD; Thompson et al. 2007) of 60 kt as opposed to the “Strong directional and speed shear near 50 kt.” The listed paper demonstrated the effectiveness of EBWD to discriminate between between supercellular and non-supercellular storms. Furthermore, I recommend the use of effective storm-relative helicity (ESRH) instead of the 0–1-km SRH. Figure 8 in Thompson et al. (2007) shows that ESRH better discriminates between significant and weak tornado environments than does 0–1-km SRH. Note that the ESRH of 528 $m^2 s^{-2}$ observed in the 1900 UTC sounding is above the 10th percentile of the sigtor distribution in their Fig. 8! There’s no question it was a strongly sheared environment, regardless of the parameter evaluated.

I’ve restructured this section substantially. I’ve not only cited Thompson et al. but also elaborated on the T07 research and lightly compared the T07 data with the 1900 observed sounding to help reflect the Pilger environment.

O17 suggested the eddies (vortices) were part of a vertical vorticity sheet (VVS) which moved southwest (in a storm-relative sense) along the FFDB. While in the general area of the SVC, I couldn’t find where they explicitly stated the eddies (vortices) were part of the SVC.

This is correct, O17 does not explicitly state that the eddies are the SVC. However, the eddies are within the VVS (017 Fig. 7), and one could assume they are likely part of the “train of vortices” which would be part of the overall SVC. As such, I’ve changed the verbiage to “the location of or very near the eddies…”. Per O17 and O18, this area, and [its] features may have significance regarding tornadogenesis.

While we have broadbrushed the SVC to include the VVS, we are not necessarily suggesting that these eddies are the “parade of vortices” within the VVS (although probable), but rather, more of a horizontal vorticity “roll”. It seems important to note that the SV2 eddy/rolls observations was some 12 min prior to the SV1 observation of tornadogenesis (from his viewpoint) and mentioned in SV1 observations in this paper. This timeframe led us to question the eddy/rolls’ location near the FFDB with respect to the VVS and the” parade of vortices”. While not referenced/cited, Orf further discusses these “rolls” in more detail during the plenary talk at CSME-CFDSC, which can be seen at the 18:10 timeframe at the link below:

Leigh Orf's plenary talk at CSME-CFDSC Congress 2019, Western University, ON

Additional discussion of the VVS and the "eddies/rolls" can be seen at 34:30–34:50, where Orf indicates the VVS "rolling up into vortices and being part of the SVC" directly. With this uncertainty, we felt that making a firm statement otherwise would be speculation, and the reason for broadbrushing the SVC.

Is it possible that the growing dust column from 17a to 17b enshrouded some of the subvortices, such that it wasn't as dramatic consolidation? Regardless, it's fascinating footage. Is it possible to edit the YouTube video to somehow highlight the times of these two screen captures? I feel like the reader would be able to better appreciate the rapid transition.

[S]ome vortices could have been enshrouded in old Fig. 17b (new Fig. 18b), after the transition, but we do not believe this is the case in Fig. 18a. I've edited a new Pilger probe video 2, annotating the vortices during this timeframe. Also, per reviewer A request, I have also increased figure sizes, which we believe clearly show the nine "mini" closed vortices. I have also added another figure (Fig. 19) to reflect the estimated location and position of the vortices from the probe viewpoint, to cross-reference Fig. 18. We believe this will help the reader visualize the position of the vortices with respect to the two-dimensional plane view of Fig. 18.

[The 21:09:28 video frame and associated video clip] Another incredible video capture. However, the numbering and lettering seem somewhat arbitrary from just the still image. For example, there are two distinct vortex tubes emerging from the top of the dust shroud on the north side of the broader vortex. Are both of those considered "1", or are they "1" and "2"? I would encourage the authors and the editor to provide full-resolution links to the imagery so the reader can really hone in on some of these features.

This is a good question and one we pondered for a long time. The timetable for writing this manuscript took years, as we spent over 28 months going over twelve thousand video frames alone. We sought outside assistance from another video engineer from Cox Communications in Tulsa, OK, as well as two outside meteorologists, and two video brokers to assist with the vortices count.

In this particular video frame at 21:09:38 UTC (from DT as they were escaping to the east near the Pilger Sand and Gravel Pit) we originally counted seven vortices. The two vortices in question, that are somewhat horizontal vortex tubes on the north side of the broader vortex, were ultimately removed from our count, as these vortices were "attached" or a part of the parent vortex #1. Therefore, we just counted them as one vortex. However, we believe this question also highlights our findings of vortex breakdown within vortex breakdown. Additionally, we did find numerous "mini" vortices (near double digits) prior to 21:09:35 UTC, but had reservations in our total count due to the very quick nature of these "mini" vortices. Thus, they were not included in this case study. As reviewer A requested, I have added direct links to the video.

[Minor comments omitted...]

Second Review:

Recommendation: Accept.

[Minor comments omitted...]